Analysis of Environmental and Operational Condition Effects on Guided Ultrasonic Waves in Stiffened CFRP Structures

Benjamin Eckstein, Maria Moix-Bonet, Martin Bach

7th European Workshop on Structural Health Monitoring
July 8-11, 2014. La Cité, Nantes, France

ANALYSIS OF ENVIRONMENTAL AND OPERATIONAL CONDITION EFFECTS ON GUIDED ULTRASONIC WAVES IN STIFFENED CFRP STRUCTURES

Benjamin Eckstein[1], Maria Moix-Bonet[2], Martin Bach[1]

[1] *Airbus Group Innovations, Airbus-Allee 1, 28199 Bremen*
[2] *Deutsches Zentrum für Luft- und Raumfahrt, Airbus-Allee 1, 28199 Bremen*

Benjamin.Eckstein@airbus.com

ABSTRACT

Structural Health Monitoring by Guided Ultrasonic Waves for real world applications relies on compensation of operational and environmental effects. The effects to be taken into account are depending not only on the present factors for a particular application scenario, but as well on the structure to be monitored itself. Especially for stiffened CFRP structures, wave propagation and subsequent temperature effects are of increasing complex nature. The load and temperature condition of aerospace components typically vary along the flight cycle of an aircraft and is subject of a vast number of operational and environmental factors.
The extensive research on temperature influence on wave propagation and transduction as the most important influence factor in the last years has broad up two widely spread methods for temperature compensation: Optimum Baseline Selection and Baseline Signal Stretch, which can be applied in a combination as well. In this work the existing compensation concept are challenged regarding its applicability to real world structures and environmental and operational conditions. For that purpose experimental data from two structures are analysed. Firstly, the influence of on wave propagation is analysed in the scope of a lab test by data from a stiffened CFRP panel subject to temperature variation. Secondly, the influence of environmental and operational conditions in the frame of a flight test is analysed.

KEYWORDS : *Guided Ultrasonic Waves, environmental and operational conditions.*

INTRODUCTION

The increasing usage of Carbon Fibre Reinforced Plastics (CFRP) for primary aerospace structures, such as on the A350XWB or the B787, involves to handle the principal susceptibility of composite laminates to impact loads as well as the occurrence of barely visible impact damages. As one consequence, damage tolerance design usually implies that any visible indication of impact damage needs to be assessed by NDI. Increasing the structural robustness in order to decrease maintenance costs and service interruptions, will in turn increase the weight of the structure as well. In this area of conflict, Structural Health Monitoring by Acousto Ultrasonics as an enhancement of conventional NDI offers the potential to decrease the related maintenance cost and increase the availability of the aircraft.

This paper deals with influences of environmental and operational conditions present in real world, complex structures on Guided Wave propagation and implication on the application of Acousto-Ultrasonic based SHM. The data used in here is gathered in a flight test, which has been presented in detail before, therefore the reader is kindly referred [1]. In the following common temperature compensation methods and their limitations at complex CFRP structures will be briefly reviewed, accompanied with an introduction of wavelet coherence as one signal processing technique to quantify signal variation between reference signals and current signal.

1 THEORY

1.1 Environmental and operational conditions

An overview on environmental and operational conditions can be found in previous work for an overview [1, 2]. In this work, the analysis is primarily focusing on temperature effects. Tough, other effects like humidity can have a significant influence at CFRP structures [3].

1.2 Temperature compensation

Two methods for temperature compensation are Optimum Baseline Selection (OBS) and Baseline Signal Stretch (BSS) [4], which can be applied in a combination as well. The fundamental assumption behind BSS is an equal change in group velocity for all signal components which then leads to a linearly increasing shift in time, as later components accordingly travelled a longer distance. This time shift can either be estimated via the local temporal coherence or iterative optimization of a residual criterion [5], and the baseline signal then can be globally corrected by the according stretch factor. The change due to transducer and coupling characteristics is only indirectly addressed by the OBS. [4] discusses and names limitations of BSS method, i.e. assumption of isotropic velocity changes, homogeneous temperature field, neglect of wave shape of dispersive waves. Already for isotropic plates the difference in velocity and velocity change due to temperature of the occurring two fundamental wave-modes will introduce some error.
When looking at realistic stiffened, anisotropic CFRP structures, the theoretical sources of error become more diverse:

- In the temperature range of interest, mainly the properties of the matrix of the CFRP and therefore shear and transverse stiffness are temperature dependent. Therefore it can be expected, that wave modes show larger difference in velocity changes, as the resulting out-of-plane displacement components depend much more on the matrix properties.
- Reflection at features of the structure, such as stringers, may create propagation paths with reasonable different velocity change characteristics due to anisotropy.
- Furthermore, mode conversion can create wave packages in the receiving signal which are locally subject to different velocity changes.

In summary, it is reasonable to view with care on the application of BSS for complex CFRP structures and bear in mind that a compensation method limits the overall performance of an SHM system. Unfortunately, there is no other method available overcoming the limitations, therefore it is of interest to estimate that limitation with realistic data.
It has to be noted, that the impact of the accuracy of temperature compensation of course depends as well on the chosen algorithms for damage assessment.

1.3 Local Temporal Coherence

As mentioned above local temporal coherence can be used to rate temperature induced time delay and subsequently estimate a stretch factor. Though [5] applied this method for diffuse ultrasound wave fields, it gives a useful localized information also for the non-diffuse part of a signal. First, the time-windowed correlation coefficient function is defined for signals x_1 and x_1 using time windowed estimates on cross-correlation $\hat{R}_{12}^T$, and autocorrelation $\hat{R}_{11}^T$ and $\hat{R}_{22}^T$, for further details see [5]:

$$\gamma_{12}^T(t,\tau) = \frac{\hat{R}_{12}^T(\tau,t)}{\sqrt{\hat{R}_{11}^T(0,t)\hat{R}_{22}^T(0,t)}} \tag{1}$$

Subsequently the peak coherence C_{12} and corresponding peak delay D_{12} are defined :

$$C_{12}(t) = \max_{\tau} \left| \hat{\gamma}_{12}^T(t,\tau) \right|, \tag{2}$$

$$D_{12}(t) = \arg\max_{\tau} \left| \hat{\gamma}_{12}^{T}(t,\tau) \right|. \tag{3}$$

The window length use here is set to one cycle of the excitation signal.

1.4 Cross Wavelet Transform and Wavelet Coherence

Cross Wavelet Transform (XWT) is defined as [6,7]:

$$W^{XY}(s) = W^{X}(s) W^{Y*}(s), \tag{4}$$

where W^X and W^Y denote wavelet transforms at scale s of two time series X and Y, * denotes complex conjugation. With $S(\ )$ being a smoothing-operator in time, the wavelet coherence is then further given by:

$$R^{XY} = \frac{\left| S\left(W^{XY}\right) \right|^2}{S\left(W^{XX}\right) S\left(W^{YY}\right)}. \tag{5}$$

The phase of the wavelet coherence is a measure of local phase difference:

$$\varphi = \tan^{-1}\left(\frac{\Im\left(R^{XY}\right)}{\Re\left(R^{XY}\right)} \right). \tag{6}$$

In this work, the complex Morlet wavelet as continuous wavelets transform (CWT) is utilized. Using a complex CWT allows representation of modulus and phase, see also figure 3 for an example. Accordingly, wavelet coherence possesses as well phase information. Both, wavelet coherence and complex CWT are implemented in the wavelet toolbox of MATLAB. From the phase difference a time delay can be calculated using the Fourier period of the utilized wavelet.
The length of the window of the smoothing operator is a sensitive parameter, as it principally counteracts the localization of the wavelet in time (and frequency) [6]. In this work the window length is set to twice the period of the centre frequency of the excitation signal.

2 EXPERIMENTAL DATA

2.1 Stiffened panel lab test data

The test data origins from a curved, omega-stringer stiffened CFRP panel of constant thickness. Measurements have been taken at steps of 5 °C in the temperature range of 35 °C to 55 °C in an oven [8]. The specimen is equipped with SMART layer sensors of diameter 6.35 mm, which are placed in a regular grid of 100 mm spacing parallel to the stringers and ca. 200 mm perpendicular to the stringer (i.e. the stringer pitch). For the purpose of demonstration a signal of transducer pair creating a propagation path diagonal across the stringer is chosen. These signals are displayed in figure 1.

2.2 Flight test data

The flight test and the structure are in detail described in [1]. For the sake of brevity, it is just noted that the test structure is an omega-stringer stiffened CFRP fuselage panel of equal thickness. The regular grid of sensors has a pitch of 100 mm parallel and ca. 200 mm perpendicular to the stringers. Again SMART layer sensors are used with transducers diameter of 6.35 mm.
A subset of the datasets described in [1] is selected for analysis in this work as stated in the legends of the following figure by the numbers with a preceding hash sign. For the purpose of demonstration again a signal of transducer pair creating a propagation path diagonal across the stringer is chosen. These signals are displayed in figure 2.

3 RESULTS

3.1 Results of stiffened panel lab test data

Figure 1 below shows the signals at five different temperatures as well as the peak coherence and time delay of the signal at 45 °C to the other four signals. The centre frequency of the excitation signal is 180 kHz.

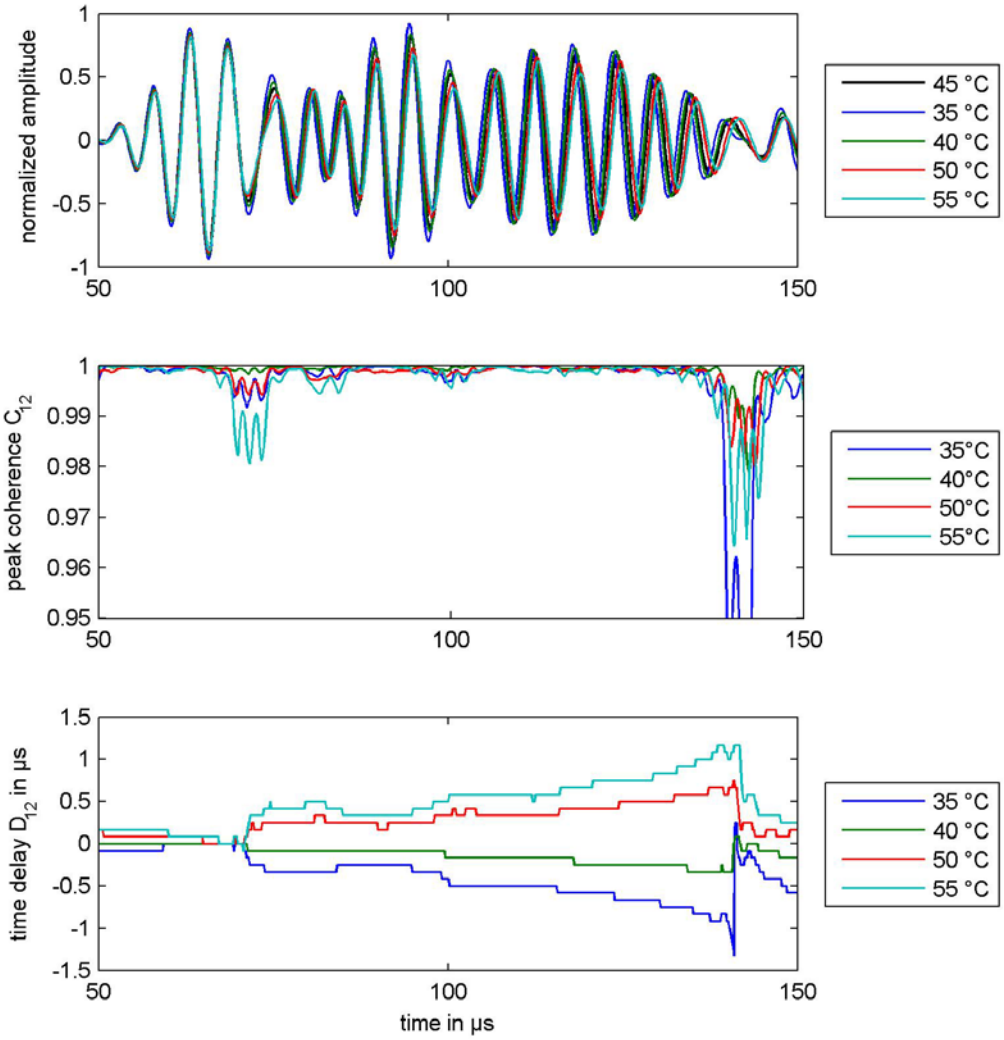

Figure 1: Exemplary signal from lab test at different temperatures (top), peak coherence (middle) and according peak delay (bottom)

It can be seen in figure 1 that there is an approximately linear change of time delay over time, with an actual lag (positive delay) for positive temperature difference and a lead (negative delay) for negative temperature difference. Clearly, the linear change increases with temperature difference.
Furthermore it has to be noted, that the signals show interfering wave packages. The sections with strong change of the interference show a drop in coherence and a larger distortion in the time delay curve. In order to avoid an adverse impact of such distortion, a calculation of the stretch factor can be limited to the parts with sufficient coherence [5].
Applying a linear stretch will primarily introduce errors at the sections with low coherence due to interference, as the time delay curves show larger deviation from linear changing behaviour.

Therefore the temperature difference needs to be small enough to avoid loss of coherence at the sections of interfering wave packages.

3.2 Results of flight test data

Figure 2 shows the signals at seven different temperatures as well as the peak coherence and time delay of the signal at 22 °C to the other six signals. The centre frequency of the excitation signal is 220 kHz.

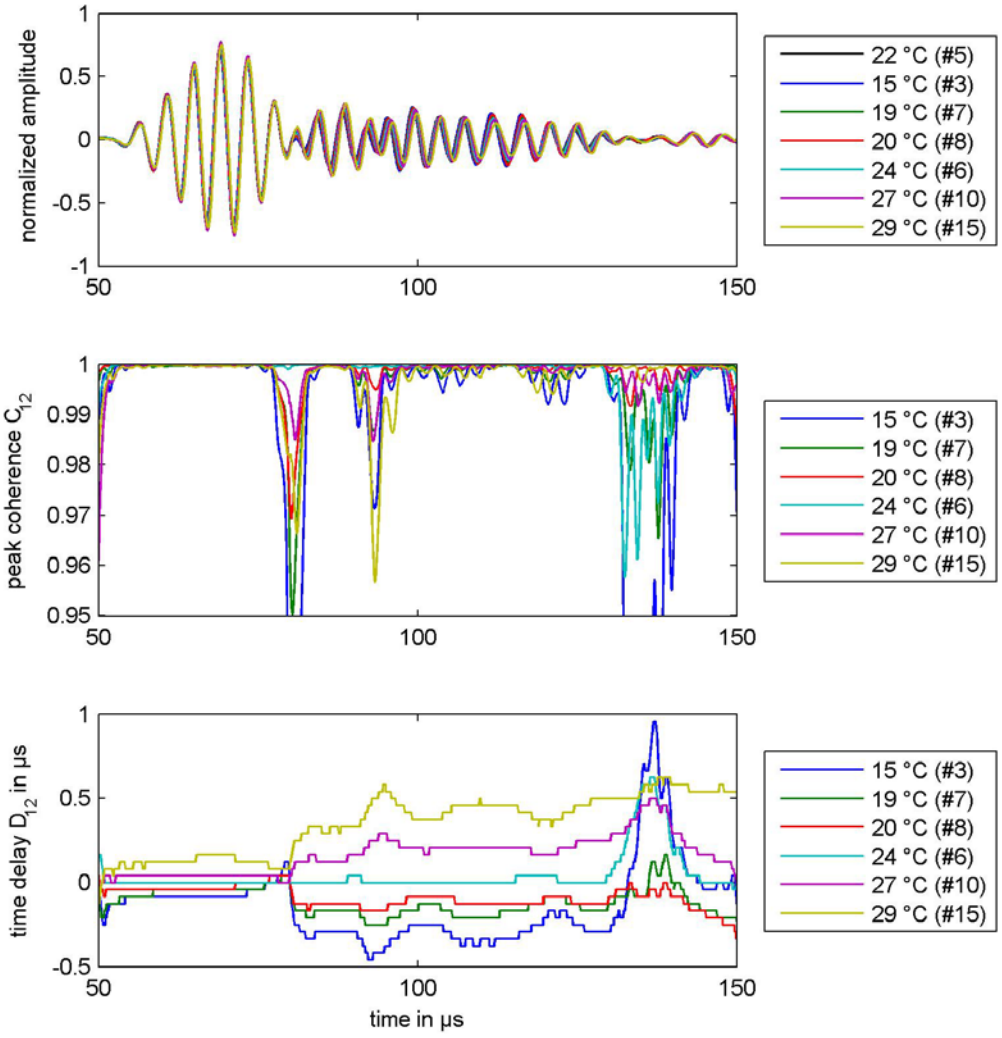

Figure 2: Exemplary signal from flight test at different temperatures (top), peak coherence (middle) and according peak delay (bottom)

Similar to figure 1, it is visible in figure 2 that there is an approximately linear changing time delay over time, which again is depending on temperature difference. In the signals of this example the loss of coherence at the interference sections is more pronounced.

Figure 3 shows the complex CWT with a Morlet wavelet of and along with two example signals (dataset #5 at 22 °C and dataset #15 at 29 °C). It has to be mentioned that the parameters of the mother wavelet, i.e. the trade-off between localisation in time and frequency, have to be determined carefully. Secondly, the choice of the wavelet should be done with regard to the signal and signal features under investigation, respectively.

Generally, a time-frequency representation allows assessment over time and frequency, thus the incorporation and utilization of varying dispersion behaviour due to environmental changes would be possible, too. However, this might implies a burden in terms of computation cost.
From the plot of modulus, as well as in the phase plot, one can see that the apparent first arrival mode is almost not dispersive. Interference between the wave packages is visible by sharp drops in the CWT modulus, as the signal shape is locally not anymore that good resembled by the shape of the mother wavelet.

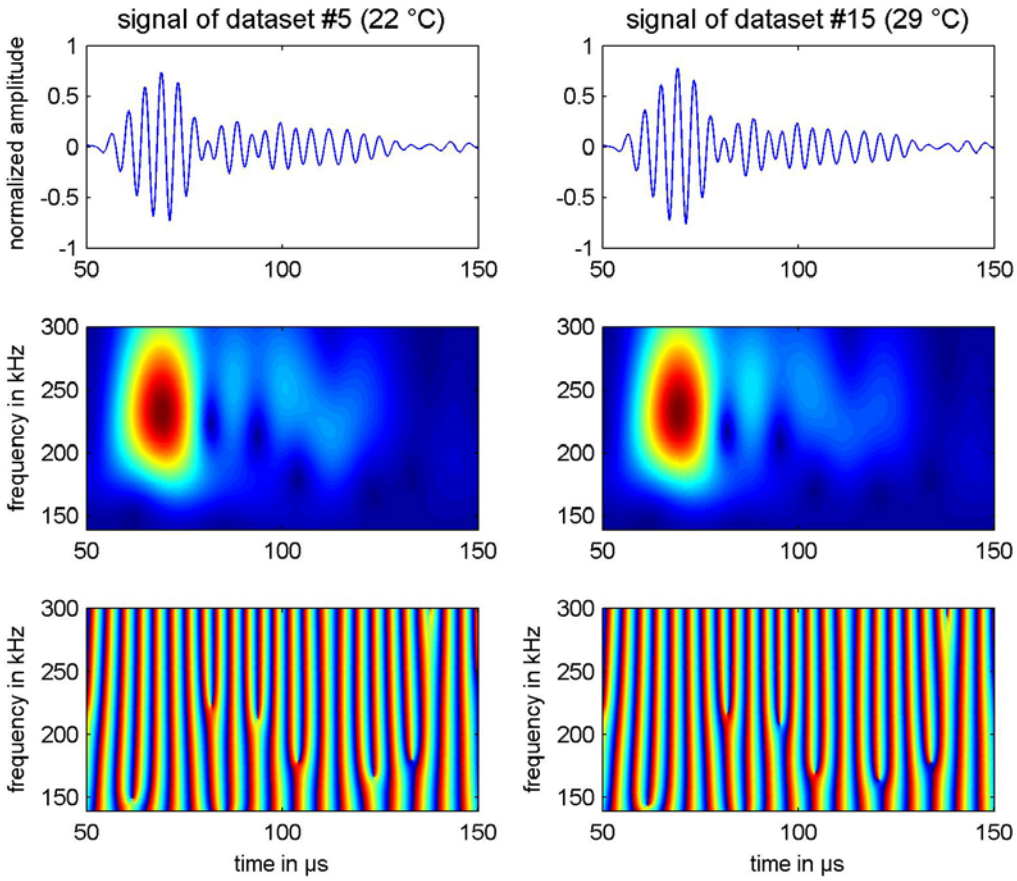

Figure 3: Exemplary signals (top), modulus of CWT (middle) and phase of CWT (bottom)

Figure 4 shows modulus and phase of the cross wavelet transform (XWT) and the wavelet coherence for the two signals used for figure 3 above. The phase of XWT (second plot form the top) is derived without smoothing in time, thus there are pronounced artefacts at points of low coherence are apparent, compare also with plot of modulus of wavelet coherence the . These artefacts are partially suppressed by the smoothing in the calculation of wavelet coherence (bottom plot), note the different scaling of the colour map. Therefore the plot of wavelet coherence phase visualises better the increase in phase difference of time alike the observation made with local time coherence.

Figure 5 shows the time delay calculated from the phase difference of XWT and wavelet coherence, respectively. For that purpose, only one slide at the centre frequency of the excitation signal is used. As visible from figure 3 and 4, this is not necessarily the frequency with peak signal energy or XWT. The smoothing at wavelet coherence calculation eases the interpretation of the delay curves. However, if only the data above a wavelet coherence (modulus) threshold value is regarded, the difference to the information from XWT phase is actually negligible. The choice of threshold value

should be made with respect to the other signal processing parameter, esp. the window length of the smoothing operator.

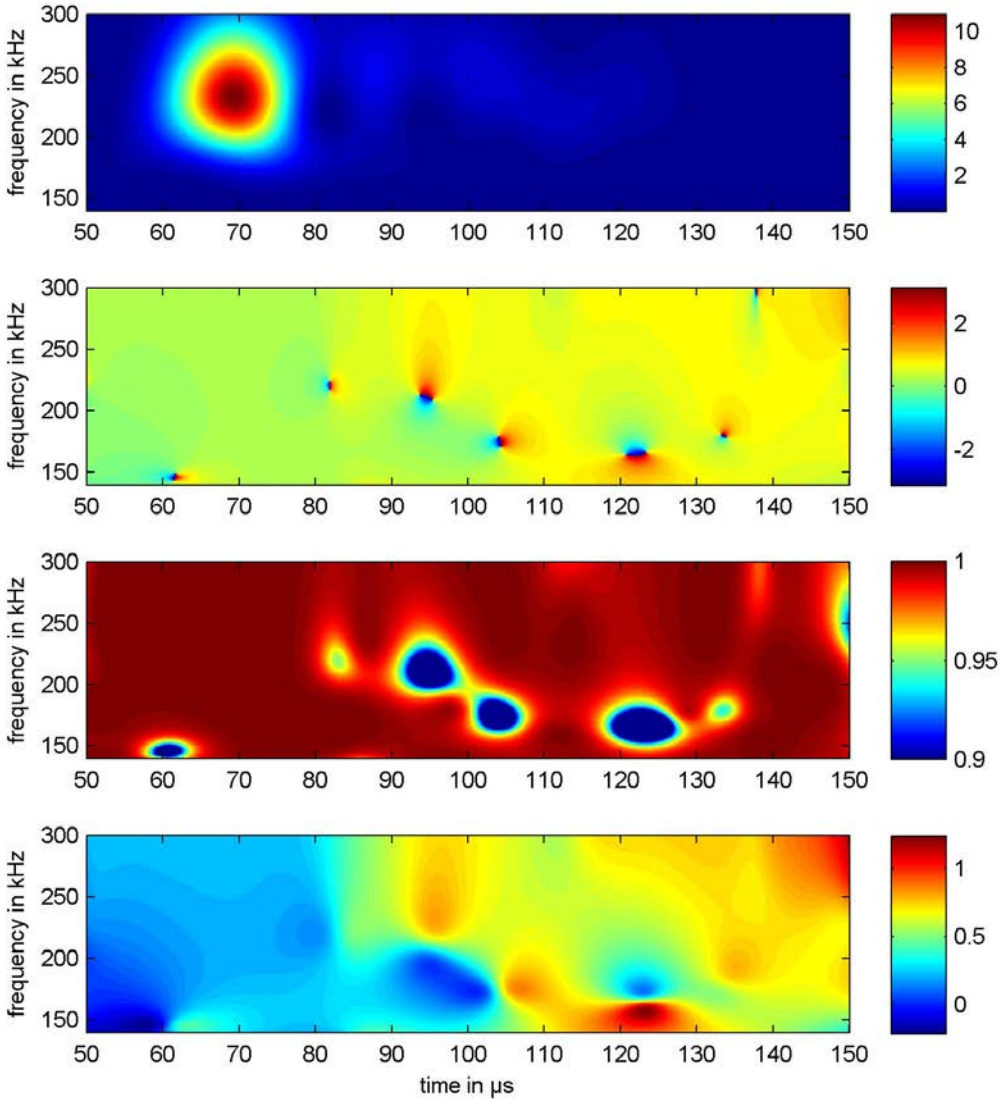

Figure 4: Modulus and phase of XWT (upper half) and modulus and phase of wavelet coherence (lower half)

With the time delay derived via complex CWT, XWT and wavelet coherence as in figure 5, one can perform BSS (and possible OBS) by estimating a linear stretch factor or iteratively maximizing the sum of XWT-modulus or wavelet coherence.
A further idea is the application of a phase change to the CWT coefficients in order to subsequently either create a time signal by inverse transform or work in the following steps of damage assessment with CWT coefficients only.

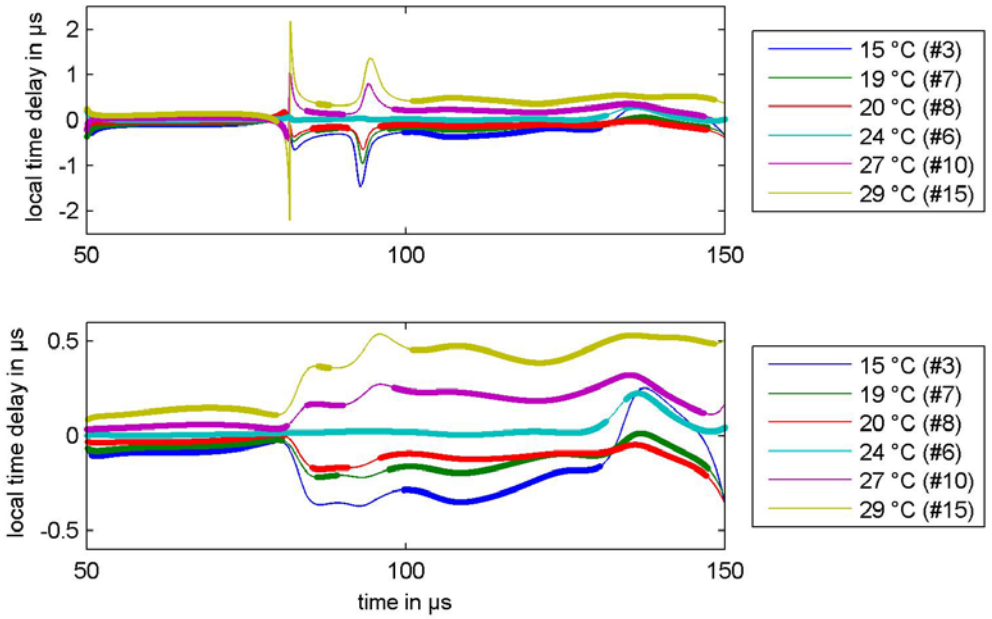

Figure 5: Time delay derived from phase of WXT (top) and time delay derived from phase of wavelet coherence (thick line corresponds to wavelet coherence higher than 0.99)

CONCLUSION

Baseline signal stretch, though theoretically not designed to be applied on anisotropic problems, can still provide useful results for such cases, as long as the temperature difference is relatively small and the interference of wave packages is not too pronounced.
As an alternative to the calculation of the stretch factor via local temporal coherence or estimation by minimization of a residual criterion, the time delay from wavelet cross transformation or wavelet coherence phase based on complex continuous wavelet transform is presented.

REFERENCES

[1] Eckstein, B., Bach M., Bockenheimer C., Cheung C., Chung H., Zhang D., Li F., Large Scale Monitoring of CFRP Structures by Acousto-Ultrasonics – A Flight Test Experience, 2013, *Proceedings of the 9th International Workshop on Structural Health Monitoring 2013,* pp. 528-535.

[2] Eckstein, B., Fritzen, C.-P., Bach, M., Considerations on the Reliability of Guided Ultrasonic Wave-Based SHM Systems for CFRP Aerospace Structures, 2012, *Proceedings of the 6th European Workshop on Structural Health Monitoring 2012,* pp.957-964.

[3] Schubert, K., Brauner, C., Herrmann A., Non-damage-related influences on Lamb wave-based structural health monitoring of carbon fiber reinforeced plastic structures, *Structural Health Monitoring* (2014) Vol. 13(2): 158-176.

[4] Croxford, A., Moll, J., Wilcox P., Michaels, J., Efficient temperature compensation strategies for guided wave structural health monitoring, *Ultrasonics* 50 (2010) 517-528

[5] Michael, J.E., Michaels, T., Detection of Structural Damage from the Local Temporal Coherence of Diffuse Ultrasonic Signals, *IEEE Transactions on Ultrasonics, Ferroelectrics, and Frequency Control*, Vol. 52(10): 1769-1782, 2005.

[6] Torrence, C. and Compo, G. P.: A practical guide to wavelet analysis, *Bull. Am. Meteorol. Soc.* 79 (1998): 61-78.

[7] Grinsted, A., Moore, J. C. and Jevrejeva, S.: Application of the cross wavelet transform and wavelet coherence to geophysical time series, *Nonlinear Processes in Geophysics* 11 (2004): 561-566.

[8] Moix-Bonet, M., Processing of Acousto-Ultrasonic Data for analysis of temperature parameters and damage detection in CFRP Structures, diploma thesis, Universität des Saarlandes, 2011.